the negative chirality conferred by the coupling path III-I-IV. Mason's conjecture[5] is discernible in the 3s Rydberg excitations in both DMC and TMC: the II-V coupling in DMC is positive in both 1A and 2B, while the III-IV coupling in TMC (1B) is negative and the III-VI and IV-VII couplings are positive. This rule does not hold for the 3p Rydbergs, however, and in the 2B excitation of DMC, it does not determine the sign.

V. Concluding Remarks

The RPA in extended basis set calculations is capable of giving a good account of low-lying singlet electronic excitations, both in terms of energies and of oscillator and rotatory strengths. Even with basis sets of the size used here, however, one cannot claim that further basis optimization would not yield further improvement. Beyond that, the systematic overestimation of excitation energies, as compared with our previous work on planar monoolefins,[19] shows that higher-order effects are important for these strained-ring systems. As regards the stereochemical "puzzle" of DMC vs. TMC, the present calculations show that the long-wavelength CD bands are of different nature in the two molecules so that sign correlations are not to be anticipated. Because of the high density of states in cyclopropane and its derivatives, perhaps some caution is appropriate in assigning absolute configurations solely on the basis of correspondence of long-wavelength CD in these molecules.

Acknowledgment. Acknowledgment is made to the donors of the Petroleum Research Fund, administered by the American Chemical Society, for support of this research. This work was also supported in part by the National Science Foundation (CHE-82-18216). We thank the Data Processing and Computing Center of Southern Illinois University at Edwardsville for generous grants of computer time. Finally, we are grateful to Profs. Harry Morrison and William Jorgensen for providing us with a copy of the contour plot program, which we have adapted for PROGRAM RPAC.

(20) Bouman, T. D.; Hansen, Aa. E. *Chem. Phys. Lett.* **1985**, *117*, 461-467.
(21) (a) Jorgensen, W. L.; Salem, L. *The Organic Chemist's Book of Orbitals*; Academic: New York, 1973. (b) Morrison, H.; Jorgensen, W. L.; Bigot, B.; Severance, D.; Munoz-Sola, Y.; Strommen, R.; Pandey, B. *J. Chem. Educ.* **1985**, *62*, 298-301.

Oxygen Transfer from Iron Oxo Porphyrins to Ethylene. A Semiempirical MO/VB Approach

A. Sevin*† and M. Fontecave‡

Contribution from the Laboratoire de Chimie Organique Théorique, UA N° 506 CNRS, Bâtiment F, 75232 Paris, Cedex 05, France, and the Laboratoire de Chimie et Biochimie Pharmacologiques et Toxicologique, UA N° 400 CNRS, 75270 Paris, Cedex 06, France. *Received March 18, 1985*

Abstract: A semiempirical study of oxygen transfer from oxo porphyrins to ethylene is proposed, based on EHT calculations augmented by VB analysis of the resultant wave functions. It is shown that the Fe^{IV}–O chromophore bears a substantial radical character ($Fe–O^0$) and thus reacts like an RO^0 species. MO and state correlation diagrams are used in order to underline the major electronic events found along the various pathways. An interplay between adiabatic surfaces of even d^n configurations allows for the obtention of resultant diabatic surfaces corresponding to one-electron-transfer mechanisms. It is shown that the observed stereoselectivity results from the competition between potential energy barriers and rotation around the C–C bond in the intermediate radical. A qualitative VB picture of the reactivity is proposed which emphasizes the role of spin polarization.

Cytochrome P-450 monooxygenases catalyze the reductive activation of dioxygen by NADPH[1] and the insertion of one oxygen atom into various organic bonds such as in alkanes or alkenes according to the scheme below. The fact that exogenous

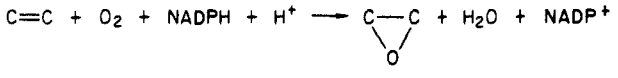

oxygen donors such as alkyl hydroperoxides[2] and iodosylbenzene[3] are effective oxygen atom sources for the hemoprotein in the absence of O_2 and a reducing agent has supported the view that the active transient species is an electrophilic oxoiron complex.[1] Two types of complexes have been considered: an iron(V) oxo complex **1** or an iron(IV) oxo porphyrin cation radical **2**.[1] In

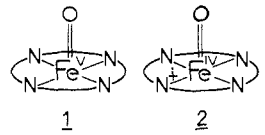

1 2

favor of structure **2** is the recent report that this radical is formed at low temperature upon the heme model reaction of an iron(III) porphyrin with iodosylbenzene or peroxybenzoic acid.[4] This species is able to efficiently epoxidize alkenes and has therefore been postulated as the active oxygen complex in the model oxidation of hydrocarbons catalyzed by synthetic iron porphyrins.[5] Several other ferryl complexes have been reported: (i) On the grounds of spectroscopic data, **2** has been shown to be a key intermediate in the mechanism of action of peroxidases (compound I of horseradish peroxidase (HRP) and catalase.[6,7] (ii) A por-

† Laboratoire de Chimie Organique Théorique.
‡ Laboratoire de Chimie et Biochimie Pharmacologiques et Toxicologique.

(1) Ulrich, V. *Top. Curr. Chem.* **1979**, *83*, 68.
(2) Nordblom, G. D.; White, R. E.; Coon, M. J. *Arch. Bichem. Biophys.* **1976**, *175*, 524.
(3) Ulrich, V.; Ruf, H. H.; Wende, P. *Croat. Chem. Acta* **1977**, *49*, 213.
(4) Groves, J. T.; Haushalter, R. C.; Nakamura, N.; Nemo, T. E.; Evans, B. J. *J. Am. Chem. Soc.* **1981**, *103*, 2884.
(5) (a) Groves, J. T.; Nemo, T. E.; Myers, R. S. *J. Am. Chem. Soc.* **1979**, *101*, 1032. (b) Groves, J. T.; Kruper, W. J.; Nemo, T. E.; Myers, R. S. *J. Mol. Catal.* **1980**, *7*, 169. (c) Chang, C. K.; Kuo, M. S. *J. Am. Chem. Soc.* **1979**, *101*, 3413. (d) Change, C. K.; Ebina, F. J. *J. Chem. Soc., Chem. Commun.* **1981**, 778. (e) Mansuy, D.; Bartoli, J. F.; Momenteau, M. *Tetrahedron Lett.* **1982**, *23*, 2871. (f) Lindsay-Smith, Sleath, P. R. *J. Chem. Soc., Perkin Trans. 2* **1982**, 1009. (g) Groves, J. T.; Nemo, T. E. *J. Am. Chem. Soc.* **1983**, *105*, 5786. (h) Groves, J. T.; Myers, R. S. *Ibid.* **1983**, *105*, 5791. (i) Groves, J. T.; Nemo, T. E. *Ibid.* **1983**, *105*, 6243.

0002-7863/86/1508-3266$01.50/0

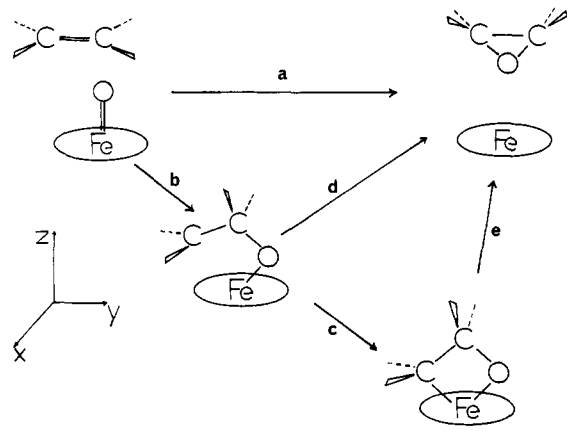

Figure 1. General reaction scheme. The *yz* plane is taken as a symmetry element.

phyrin-Fe^{IV}-O (S = 1) structure has been proposed for the compound II of HRP as well as for the product derived from the reaction of hydrogen peroxide with myoglobin.[8] (iii) A heme model ferryl complex has been recently prepared by the reaction of a porphyrin-Fe^{III} peroxo-bridged dimer with nitrogenous bases and found able to oxidize triphenylphophine at −80 °C.[9-11] (iv) It is noted that non-porphyrin Fe^{IV} oxo complexes have been postulated as reactive species in aliphatic hydroxylation by the hydrogen peroxide–ferrous ion.[12,13]

The mechanism of oxygen transfer from cytochrome P-450 or heme model Fe–oxo complexes to alkenes, yielding epoxides, has been widely investigated. Very recently, several authors have proposed the intermediate formation of a metallacycle **3** through the nonconcerted addition of the reactive species to the double bond,[14-16] in agreement with the stereospecificity of the reaction.[5a,b,f,g] (See Figure 1, paths b and c). This unstable inter-

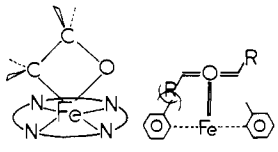

3 4

mediate complex yields the epoxide via reductive elimination of two cis ligands (Figure 1, path e). Moreover, Groves et al.[5g] have proposed the geometry of structure **4** for the attachment of the double bond to Fe–O. Such an approach, where the alkene plane is perpendicular to the porphyrin ring, reveals steric interactions between the olefin substituents and those of the porphyrinic moiety and accounts for the greater reactivity of cis olefins with respect

Chart I. Structures Used in the EHT Calculations[a]

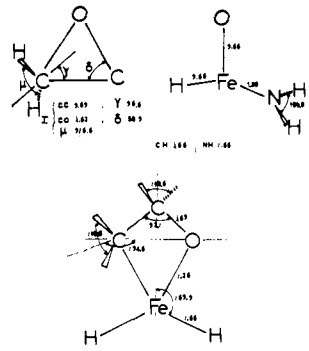

[a] Epoxide II with an isoceles geometry has been used for scanning the formation and evolution of the metallacycle. The EHT parameters for C, O, H, and N are standard; for Fe they are H_{3d} = −12.7, exp = 5.35 and 1.8; contraction coefficients, 0.5366 and 0.6678; H_{4s} = −9.17, exp = 2.275; H_{4p} = −5.37, exp = 2.275.

to the trans isomer observed in iron(III) porphyrin–iodosylbenzene systems.[5g] The bonding and electronic properties of ferryl complexes have been previously studied by using semiempirical calculations[17-21] and ab initio techniques,[22-24] but no theoretical treatment of their reactivity toward alkenes is available. This paper reports a semiempirical theoretical investigation of the series of reactions shown in Figure 1. In this exploratory attempt, our goal is to outline the great variety of problems that arise and to provide a guideline for further more quantitative studies.

Model Reaction Paths and Methodology

A general scheme for the study of iron oxo porphyrin reactivity is given in Figure 1, where limiting reaction paths are proposed. Reaction a consists in direct extrusion of oxygen, yielding ethylene oxide and a Fe porphyrin. The same final system may be obtained through a stepwise process consisting of path b, leading to an intermediate moiety, for which paths c and d are competitive evolution channels. Via path e, the metallacycle is cleaved through the synchronous rupture of two bonds. In order to theoretically study these reactions, we have used the general framework of the Extended Hückel theory (EHT)[25] for building up a *localized* VB description of the Fe–O chromophore. In this aim, we just required realistic coefficients for the relevant atomic orbitals of Fe and O, in a selected set of MOs. It is well-known that the relative magnitude of these coefficients is not likely to vary noticeably in valence MOs with the obtention method, provided that we used a double-ζ quality basis set for the iron atom. In this perspective, the porphyrin ring is considered as imposing its symmetry field to the Fe–O unit and is also assumed to remain unchanged in the first step of the reaction. The latter point obviously constitutes a first-order approximation but can be comforted by the fact that non-porphyrin systems such as $FeCl_3$ have been shown to catalyze the epoxidation of alkenes by iodosylbenzene.[2] Even taking into account these restricted requirements, we have had to use simplified model structures. Several have already been proposed.[22,23,26]

(6) Henson, W. D.; Hager, L. P. In *The Porphyrins*, Dolphin, D., Ed.; Academic: New York, 1979; Vol. 7.
(7) Morishima, I.; Takamuki, Y.f Shiro, Y. *J. Am. Chem. Soc.* **1984**, *106*, 7666.
(8) La Mar, G. N.; de Ropp, J. S.; Latos-Grazynski, L.; Balch, A. L.; Johnson, R. B.; Smith, K. M.; Parish, D. W.; Cheng, R. J. *J. Am. Chem. Soc.* **1983**, *105*, 782 and references 1–13 cited therein.
(9) Chin, D. H.; Balch, A. L.; La Mar, G. N. *J. Am. Chem. Soc.* **1980**, *102*, 1446.
(10) Chin, D. H.; Balch, A. L.; La Mar, G. N. *J. Am. Chem. Soc.* **1980**, *102*, 5945.
(11) Balch, A. L.; Chan, W.; Cheng, R. J.; La Mar, G. N.; Latos-Grazynski, L.; Renner, M. W. *J. Am. Chem. Soc.* **1984**, *106*, 7779.
(12) Groves, J. T.; McClusky, G. A. *J. Am. Chem. Soc.* **1976**, *98*, 859.
(13) Groves, J. T.; Van der Puy, M. *J. Am. Chem. Soc.* **1976**, *98*, 5290.
(14) Sheldon, R. A. *J. Mol. Catal.* **1983**, *20*, 1.
(15) (a) Mansuy, D.; Leclaire, J.; Fontecave, M.; Momenteau, M. *Biochem. Biophys. Res. Commun.* **1984**, *119*, 319. (b) Mansuy, D.; Leclaire, J.; Fontecave, M.; Dansette, P. *Tetrahedron* **1984**, *40*, 2847.
(16) Several intermediate metallacycles have already been proposed: (a) Sharpless, K. B.; Teranishi, A. Y.; Bäckvall, J. E. *J. Am. Chem. Soc.* **1977**, *99*, 3120. (b) Rappé, A. K.; Goddard, W. A., III. *Ibid.* **1980**, *102*, 5115; (c) **1982**, *104*, 448. (d) Collman, J. P.; Kodadek, T.; Rayback, S. A.; Meunier, B. *Proc. Natl. Acad. Sci. U.S.A.* **1983**, *80*, 7039.
(17) Tatsumi, K.; Hoffmann, R. *Inorg. Chem.* **1981**, *20*, 3771.
(18) Hanson, L. K.; Chang, C. K.; Davis, M. S.; Fajer, J. *J. Am. Chem. Soc.* **1981**, *103*, 663.
(19) Loew, G. H.; Herman, Z. S. *J. Am. Chem. Soc.* **1980**, *102*, 6173.
(20) Bach, R. D.; Wolber, G. J.; Coddens, B. A. *J. Am. Chem. Soc.* **1984**, *106*, 6098.
(21) Loew, G. H.; Kert, C. J.; Hjelmeland, L. M.; Kirchner, R. F. *J. Am. Chem. Soc.* **1977**, *99*, 3534.
(22) Strich, A.; Veillard, A. *Theoret. Chim. Acta* **1981**, *60*, 379.
(23) Strich, A.; Veillard, A. *Nouv. J. Chim.* **1983**, *7*, 347.
(24) Pudzianowski, A. T.; Loew, G. H.; Mico, B. A.; Branchflower, R. V.; Pohl, L. R. *J. Am. Chem. Soc.* **1983**, *105*, 3434.
(25) Hoffmann, R. *J. Chem. Phys.* **1963**, *39*, 1397. Hoffmann, R.; Lipscomb, W. N. *Ibid.* **1962**, *36*, 2179; **1962**, *37*, 2872.
(26) Tatsumi, K.; Hoffmann, R. *J. Am. Chem. Soc.* **1981**, *103*, 3328 and references cited therein.
(27) (a) Fontecave, M.; Mansuy, D. *J. Chem. Soc., Chem. Commun.* **1984**, 879. (b) van Atta, R. B.; Franklin, C. C.; Valentine, J. S. *Inorg. Chem.* **1984**, *23*, 4121.

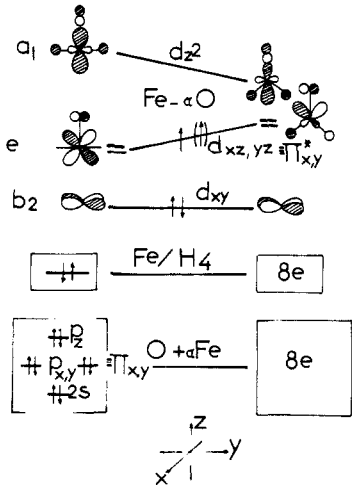

Figure 2. MOs of model H_4FeO^{2-}. In the left part, we have the situation for ∠O–Fe–H = 90°. Going to the right are shown the MO variations upon bending of this angle, preserving a C_4 axis (C_{4v} symmetry).

A first approximation is made by replacing the porphyrin ring by the simpler system **5**, where only four NH_2 are linked to Fe.[26]

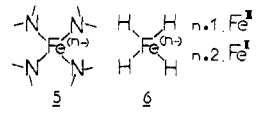

5 6

An even simpler model can be used, which only emphasizes the role of the central σ field, as in **6**, where the N atoms have been replaced by hydrogens. As far as topological and qualitative arguments are concerned, the sequential examination of **6**, and then **5**, affords a flexible tool for describing the main trends. We have verified that the MOs which were used in our VB treatment behave in a parallel fashion for both models. Several attempts have been made for optimizing the metallacycle shape. The Fe atom has been located 0.5 Å above the four-ligands plane, as found in many experimental geometries.[28] The geometry of ethylene oxide was taken from a previous study.[29] In order to delineate the various electronic features encountered along the model reaction paths, an EHT exploratory scan was first achieved, but it will not be reported here in detail. We have mainly focused our attention on the analysis of the first step of the reaction sequence, i.e., path b, and therefore, EHT arguments will only be recalled for topological reasons or for electron counting. The geometrical and EHT parameters are given in Chart I.

Since the reactivity study is centered around the Fe–O linkage, it is necessary to both make a correct description of this isolated bond and to allow for a simple analysis of the oxygen transfer.

Strictly speaking, it is difficult to depict the Fe–O unit in local terms, for in the actual wave function, Fe and O contributions are spread over a great number of MOs, delocalized on the whole skeleton. For this reason, we have combined the classical MO pictures with a qualitative VB description of the Fe–O bond. The latter method consists in transforming the molecular wave function into atomic contributions of Fe and O. This emphasizes the covalent (radical) or ionic character of these atoms, in various electronic states of the system. (See the Appendix for details.) We thus have another way of looking at Fe–O, in a localized fashion, which yields information on the electronic density around these centers.

Fe–O Bond

(a) MOs. The MOs of **6** are general enough to be used for this description. They are schematically shown in Figure 2 where they have been divided into three sets: (i) the Fe–ligand bonding set, composed of four levels occupied by eight electrons, mainly located around the ligands; (ii) four MOs bearing a dominant O character along with minor in-phase contributions of the adequate d levels of Fe; and (iii) the frontier d MOs of Fe. The $d_{x^2-y^2}$ component is antibonding and found at high energy; d_{xy} which is unperturbed, lies at the energy of the isolated atomic d level. Then we have a couple of degenerate d MOs, d_{xz} and d_{yz}, containing out-of-phase contributions of the related $2p_x$ and $2p_y$ levels of O. Finally d_{z^2} is found at slightly higher energy. These MOs and their relative energy variations upon ligand bending have already been discussed,[17] and we just have to note that the out-of-plane motion of Fe maintains the $d_{xz,yz}$ degeneracy as long as the C_{4v} geometry is preserved. The main effect of this motion is to introduce p character into these MOs, which are destabilized while d_{z^2} is stabilized to some extent. The overall destabilization remains small for moderate bending and is only 0.25 eV on going from the planar situation to an O–Fe–H angle of 107.5 which corresponds to a distance of 0.48 Å between Fe and the ligands plane. In itself, a small out-of-plane Fe motion does not noticeably change the qualitative description of the reaction paths, its main effect being to decrease the steric hindrance around the O atom and therefore to facilitate both the approach of the reactants and the possible formation of a metallacycle.

The EHT calculations yield a Fe d^4 species for Fe^{IV}–O where the O atom is surrounded by an excess of electronic density corresponding to the limiting structure L_4Fe^{4+}–O^{2-}. This description has to be improved. It must be especially noted that the MOs corresponding to the couple of unpaired electrons contain Fe and O contributions, so that the radical character is likely to be shared by both atoms. The analysis of the resulting distribution will obviously be important in dealing with the reactivity toward ethylene, since it has been shown that the active complex of the iron porphyrin–iodosylbenzene system has a free-radical character.[5]

(b) Simplified VB Description. Focusing our attention on the Fe–O bond, we see in Figure 2 that four electrons belonging to the oxygen atom are located along the z axis: two of them are found between O and Fe, having a strong O 2s contribution, and the other two point out of the Fe–O bond as a classical lone pair, of dominant O $2p_z$ character. Discarding the two electrons born by d_{xy} where neither ligand nor oxygen contribution appears, we are left with six electrons for Fe^{IV}–O or five for Fe^{V}–O distributed in two couples of degenerate MOs: O ($2p_x$ + $2p_y$) and Fe (d_{xz} + d_{yz}). Once the xz and yz planes are fixed, we can always transform, through appropriate rotation, the degenerate MOs into equivalent pure $2p_x \pm d_{xz}$ and $2p_y \pm d_{yz}$ MOs. We thus obtain two sets of orthogonal π-type bonds, both having three electrons. In that sense, the Fe^{IV}–O linkage is analogous to O_2 where the electronic situation is comparable.[30] Indeed, the electronegativity difference drains the electrons toward O, but it remains important to measure how much of the diradical character of O_2 is present in Fe^{IV}–O. In this aim, it is convenient to define the MOs that are of concern according to the shorthand notation π_x, π_y, π_x^*, π_y^*, and it is shown in the Appendix that to a first approximation, the total wave function can be written as

$$\phi = N|...\text{core}...(\Delta)|$$

where Δ is an appropriate antisymmetrized wave function containing only π and π^* terms, the remaining core behaving independently. Since in the following discussion we do not treat the energetic aspects, we can only consider the Δ Slater determinant and look at its leading features for a series of electronic states. Similar types of bonding have already been discussed by Harcourt,[31] and we will mainly emphasize the relative ionic/covalent character of the O atom. Let us take the approximate MOs as $\pi_x = 1.0[2p_x(O)] + 0.5[d_{xz}(Fe)] + \beta(L)$ and $\pi_x^* = 0.5[2p_x(O)] - 1.0[d_{xz}(Fe)] + \beta(L)$ (+ similar MOs in the yz plane) where,

(28) Smith, P. D.; James, B. R.; Dolphin, D. H. *Coord. Chem. Rev.* **1981**, *39*, 31.
(29) Bigot, B.; Sevin, A.; Devaquet, A. *J. Am. Chem. Soc.* **1979**, *101*, 1095; **1979**, *101*, 1101.
(30) Salem, L. In *Electrons in Chemical Reactions: First Principles*; Wiley: New York, 1982; p 67.
(31) Harcourt, R. D. In *Qualitative VB Descriptions of Electron-Rich Molecules: Pauling 3-electron Bonds and "Increase-Valence" Theory*; Springer-Verlag: Berlin, 1982.

Chart II. Coefficients of the VB Structures for the Case of Three Electrons in One Plane, as a Function of the Ligand Weight β[a]

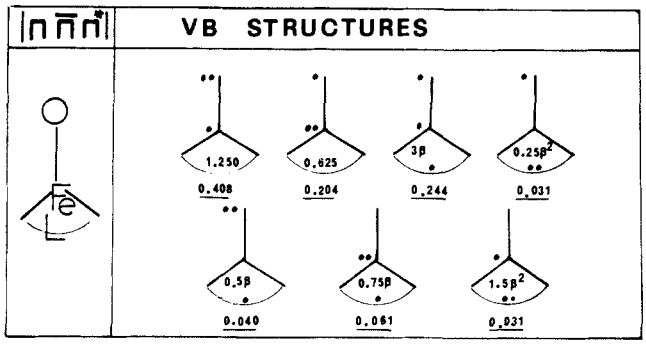

[a] Underlined are the weights obtained by setting $\beta = 0.25$. See the calculated coefficients of Table I.

apart from normalization coefficients which have been omitted, β is a small positive number that takes into account the ligand contribution. The relative coefficients of O and Fe are realistic and derive from EHT calculations.

We will first examine the case of three electrons in two such MOs. The corresponding doublet determinantal wave function is $\Delta(3) = N|\pi_x\bar{\pi}_x\pi_x^*|$, and its decomposition into O, Fe, and L contributions is given in Chart II. The terms involving L are functions of β, and it is noteworthy that when the ligand weight becomes negligible ($\beta \to 0$) the ratio covalent O/ionic O is $^1/_2$. When β increases, the term corresponding to the three unpaired electrons becomes important, thus increasing the total weight of covalent O. This is seen for the value $\beta = 0.25$, which corresponds to many calculated wave functions.

In the following sections, we have set $\beta = 0$, and π and π^* are taken equal to $\pi = 1.0[2p(O)] + \alpha[d(Fe)]$ and $\pi^* = \alpha[2p(O)] - 1.0[d(Fe)]$, where α is a positive number whose mean value is 0.5, as found in the calculated wave functions. From the examination of Chart II, we see that in doing so, we just "switch off" the ligand contributions but do not change the relative amount of the contributions having three electrons on O and Fe that are not β-dependent. This brings about a great simplification of the VB decomposition, which can be carried out easily. Several states of $\Delta(6)$ and $\Delta(5)$ have been selected. Their determinantal wave functions and the corresponding VB decomposition are given in Chart III. The numbers in parentheses are calculated weights, normalized to unity, for $\alpha = 0.5$.

Case of Fe^{IV}–O, $\Delta(6)$. The selected states are the $^3A_2$ GS of the system and its excited counterpart $^3A_2^*$ and the three singlets $^1A_1$, $^1B_1$, and $^1B_2$. Let us first remark that $^1A_1$, $^1B_1$ and $^3A_2$, $^1B_2$, whose determinantal wave functions, respectively, differ by one sign, have the same global character but of course not the same energy. Focusing our attention on the $^3A_2$ GS, we see that the O atom *has a slightly dominant covalent character*. This finding sharply contrasts with the usual fashion of "attributing" the electrons to the ligands, and concomitantly, the oxidation degree of Fe in the GS is not IV but results from the superposition of Fe^{IV} (44%), Fe^{III} (45%), and Fe^{II} (11%). On these grounds, a more flexible wave function allowing for the variation of the relative ionic-to-covalent ratio would be of the form

$$\Psi = (1 - \lambda)^3A_2 + \lambda^3A_2^*$$

The last point will bear some importance in the discussion of reactivity, since we see that this mixing—which is nothing but a 2 × 2 CI—constitutes a simple way of increasing the covalent character of the oxygen atom. The singlet states are only given for comparison and do not deserve a special discussion.

Case of Fe^{V}–O, $\Delta(5)$. The calculated VB structures of the ^2E GS (Chart III) look more complex than the preceding ones, for we now have additional possibilities involving the spatial distribution of the three electrons, with the unique restriction that their total configuration must remain doublet ($S = ^1/_2$). We see that the formal Fe^V species only has a weight of around 30%, while the structures having a covalent oxygen are dominant, the leading term being

(44%). (This notation only takes into account the electrons located in the *xz*,*yz* planes.) This description of the Fe–O linkage shows that the EHT results can be substantially improved by using a simple VB scheme. In either Fe^{IV}–O or Fe^{V}–O, the covalent character of the O atom is found to be important, and we will use this fact when studying the reactivity. In the next sections, we will examine the changes brought about by an incoming ethylene molecule to the preceding static properties.

General Considerations on the Oxygen-Transfer Reaction

To begin the study of reactivity, let us examine the hypothetical reaction whose relevant natural MO correlations[32] are given in

Chart III. V_B Structures for Fe^{IV}–O and Fe^{V}–O as a Function of α[a]

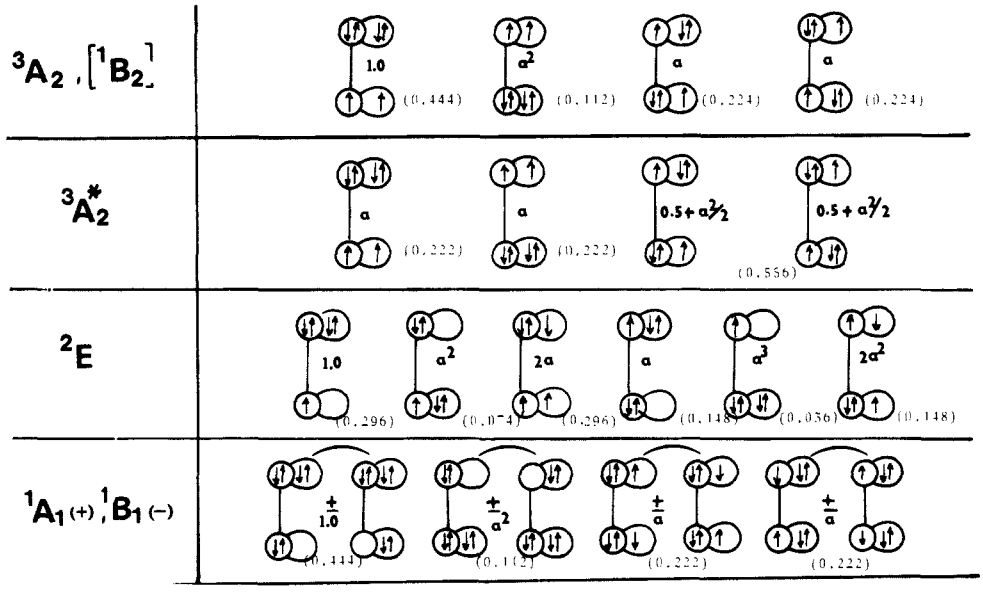

[a] See the text and the Appendix for a definition of this parameter. The values between parentheses are normalized to unity. They have been obtained for $\alpha = 0.5$ (See the coefficients of Table I.) For the ^2E state, only one-half of the wave function is drawn, the second being obtained by symmetry. The circles indicate AOs located in the *xz* plane and the ellipses AOs in the *yz* plane. The overall singlet or triplet coupling of the electrons which appears as linear combinations of spin arrangements has been reduced to one VB structure without loss of generality.

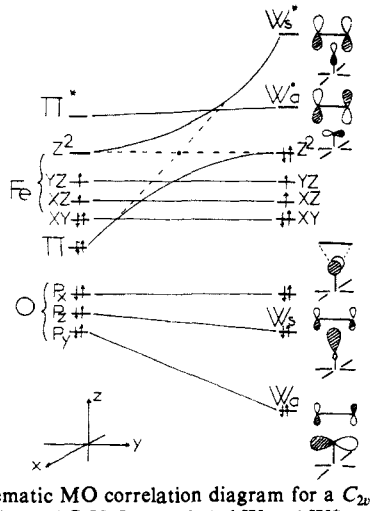

Figure 3. Schematic MO correlation diagram for a C_{2v} reaction path. The Walsh orbitals of C_2H_4O are labeled W and W* and a/s stand for antisymmetrical and symmetrical with respect to the *yz* plane.

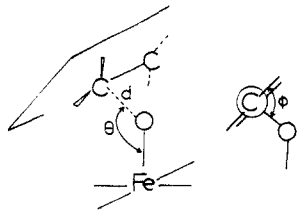

Figure 4. Parameters used in the study of the approach of the reactants.

Figure 3. They correspond to the case of Fe^{IV}–O, and for the sake of simplicity the Fe–ligands MOs have been discarded. Along this RC, the ethylene molecule approaches in a triangular geometry (C_{2v}). Even though this pathway is not the most likely, it has the merit of underlining the major electronic events that are found, at least to some extent, along any other related RC. If we just consider the system formed by C_2H_4 and the O atom, a four-electron Woodward–Hoffmann forbidden process would result:[33] the $2p_z$ level of O is correlated with a bonding Walsh orbital (Ws) of ethylene oxide, while π of C_2H_4 is correlated with the antibonding counterpart Ws*. This intended correlation is intercepted by d_{z^2} and an avoided crossing result which finally yields an allowed process. The stable $^3A_2$ GS of Fe^{IV}–O is linked to the $^3A_{2g}$ GS of the final Fe^{II} porphyrin[34] in such a way that the reaction may proceed on a single adiabatic potential energy surface (PES). Three important facts emerge: (i) The triangular approach gives rise to strong repulsive interactions. (ii) The π/d_{z^2} crossing is mediated by the oxygen atom, which possesses a minor out-of-phase contribution in d_{z^2}. (iii) The metal is reduced, $Fe^N \rightarrow Fe^{N-2}$ ($d^4 \rightarrow d^6$ or $d^3 \rightarrow d^5$), through the formal transfer of two electrons from C_2H_4 to Fe. Even though this process is "symmetry-and-spin allowed", it is clear that the local forbiddeness found between C_2H_4 and O will induce the presence of an important energy barrier along the RC.

The last three points will be used in the forthcoming discussion. We will have to find reaction paths that avoid these constraints as much as possible.

Approach of the Reactants

We have seen that the reactant approach plays an important role, and in this perspective, we have compared various geometries using C_2H_4 and **5** or **6** model compounds for either planar or pyramidalized FeL_4 fragments. In all cases, the isoceles C_{2v} approach is the most endothermic. The preferred geometry corresponds to only one carbon atom of C_2H_4 interacting with O. For a C–O distance of 2 Å, the C_{2v} geometry is at least 1.65 eV above all others. A systematic exploration of d, ϕ, θ defined in Figure 4 reveals that at short distance (1.8 Å), the potential energy curves are rather smooth upon moderate θ variation. The energy of the optimal 140° value is only 0.01 eV more stable than that of the in-line 180° geometry, the optimal ϕ dihedral angle being very close to 90° when θ varies between these limits. This result enables us to take very simple model reaction paths for our exploratory theoretical study.

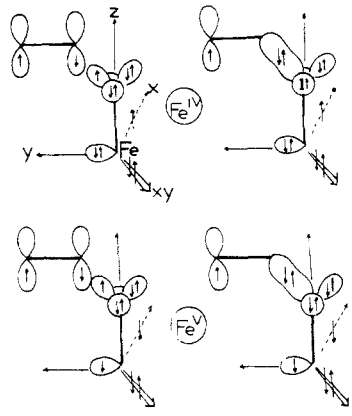

Figure 5. Qualitative VB reaction scheme, showing by continuity the various spin arrangements along the series of reactions b + c.

Qualitative VB Picture of Reactivity

The VB structures of Chart III can be used in an attempt to improve the description of reactivity. In this aim, it is noteworthy that if one only refers to the EHT/MO picture of the Fe–O bonding, the reactivity toward ethylene will be predicted to be very poor, having the essential features of an anionic RO^- addition to an alkene. This is not the case for Fe oxo porphyrins involved in oxidation of hydrocarbons, since they have been shown to react like "electrophilic species", that is, very reactive with electron-rich alkenes, and also to exhibit free-radical properties.[5] It is well established that radical additions to alkenes proceed readily, and it is clear that the more covalent the oxygen atom in our system, the easier the reaction will be, looking like RO^0 additions to alkenes. In Chart III, we have seen that the covalent character of the O atom, which is important in the $^3A_2$ GS, is enhanced upon excitation of the type $^3A_2 \rightarrow {}^3A_2^*$ or in terms of the MO located in the *xz* and *yz* planes: $|...(\pi)^2..(\pi^*)^1...| \rightarrow |...(\pi)^1...(\pi^*)^2...|$. We thus conceive that this kind of excitation provides a driving force for radical-like reactivity and can be analyzed in VB terms. Let us depict how the VB structures of ethylene can be coupled with those of Fe^{IV}–O, in order to lead to an open intermediate species. The GS of ethylene, once reduced to atomic contributions, is found to be half ionic and half covalent: $\ddot{C}_- - C_+ + C_+ - \ddot{C}_-$ (50%); $\dot{C}_\uparrow - \dot{C}_\downarrow + \dot{C}_\downarrow - \dot{C}_\uparrow$ (50%). But this solution is not optimal. It has been shown that the wave function of optimal energy, resulting from a 2 × 2 CI, having the general formula $\Psi \simeq |\pi\bar{\pi}| - \lambda|\pi^*\bar{\pi}^*|$, has the VB form $\Phi_{vb} \simeq (1 - \lambda)$ionic + $(1 + \lambda)$covalent and corresponds to $\simeq$ 80% covalent structure.[35] To a first approximation, the ethylene molecule can be considered as having a very dominant VB structure $\dot{C}_\uparrow - \dot{C}_\downarrow$ in its singlet GS. Let us now examine the coupling of two electrons of opposite spins when one ethylenic carbon interacts with O of Fe–O. The leading interaction occurs between the electrons forming the bond, and as the reaction proceeds, a concomitant polarization of all the other spins arises as it has been shown for radical additions to alkenes.[36] Once the

(32) (a) Devaquet, A.; Sevin, A.; Bigot, B. *J. Am. Chem. Soc.* **1978**, *100*, 2009. (b) Sevin, A.; Chaquin, P. *Nouv. J. Chim.* **1983**, *7*, 353.
(33) Woodward, R. B.; Hoffmann, R. *The Conservation of Orbital Symmetry*; Academic: New York, 1970.
(34) Rohmer, M. M. *Chem. Phys. Lett.*, in press.
(35) Hiberty, P. C.; Ohanessian, G., unpublished results.
(36) (a) Matsen, F. A. *J. Chem. Phys.* **1964**, *68*, 3282. (b) Fujimoto, H.; Yamabe, S.; Minato, T.; Fukui, K. *J. Am. Chem. Soc.* **1972**, *94*, 9205. (c) Salem, L.; Rowland, C. *Angew. Chem., Int. Ed. Engl.* **1972**, *11*, 92. (d) Yamaguchi, K. *Chem. Phys. Lett.* **1974**, *28*, 93. (e) Yamaguchi, K.; Fueno, T. *Ibid.* **1976**, *38*, 52. (f) Nagase, S.; Takatsuka, T.; Fueno, T. *J. Am. Chem. Soc.* **1976**, *98*, 3838. (g) Bonacic-Koutecký, V.; Koutecký, J.; Salem, L. *Ibid.* **1977**, *99*, 84. (h) Sevin, A.; Yu, H. T.; Evleth, E. *J. Molec. Struct. Theochem.* **1983**, *104*, 163.

C···O paired electrons interact, the spin polarization in some way "freezes" the spin arrangement on the other centers, and starting from a given VB structure, it is possible to anticipate, by continuity, the spin situation that will exist in the final moiety. This is shown in Figure 5 for the reactions of two covalent structures of Fe^{IV}–O and Fe^{V}–O. The paired and free electrons have been located in directional hybrids in order to pictorially emphasize their relationship in the C–O-bonded intermediate. Two oxygen lone pairs are frozen, and we assume that the reaction which occurs in the *yz* plane does not perturb the electronic features in the *xz* plane too much.

VB Scheme for the Reaction of Fe^{IV}–O. Let us focus our attention on the C–O axis. We have necessarily one electron of a given spin, say β, coming from the π system of C_2H_4, so that a potentially reactive VB structure of Fe^{IV}–O must have only one electron of a α spin around O, in the *yz* plane. All these requirements are satisfied by the VB structure having a weight of α in Chart III. The spin-freezing of this structure leads to the formation of one covalent bond along the C–O direction and leaves two unpaired electrons of α spin, one located on the terminal carbon atom, the other in d_{xz}, labeled "x" for convenience in the drawing. Two conclusions can be reached: (i) The C–O bond formation is not spontaneous since only a part of the total wave function has the correct "reactive spin arrangement", thus necessitating excitation energy for adapting the other spins to that situation. (ii) In other words, the latter process corresponds to an activation energy. Moreover, we see that the weight of the reactive VB structure is greatly enhanced in $^3A_2^*$, so that its mixing with $^3A_2$ provides an efficient way of promoting the reaction. Indeed, in state language, this corresponds to a 2 × 2 CI similar in nature to the aforementioned one, which yields the best singlet GS of ethylene. The mixing of $^3A_2$ and $^3A_2^*$ also increases the relative weight of d^5 configuration for Fe, and we have seen that this configuration is a diabatically linked to the GS of the open intermediate. More information can be extracted from this scheme dealing with the metallacycle formation: the ring closure of the open intermediate is not directly possible for two reasons: (i) We have three electrons in the *yz* plane, and the approach of the free carbon extremity to Fe will give rise to repulsive electron interaction (only two are required for forming a bond). (ii) The second unpaired electron lies in the *xz* plane with the wrong spin (triplet arrangement), and ring closure will necessitate one spin inversion. The metallacycle formation will only be possible if the electronic distribution around Fe is changed, in order to yield one electron of β spin in d_{yz}, and the corresponding process is nothing but a local excitation which is likely to be more or less endothermic and at any rate will require some time, thus allowing the intermediate to exist, at least, as a transient species.

VB Scheme for the Reaction of Fe^{V}–O. As in the preceding case, we have to select the VB structure of the GS which is the best candidate for forming a covalent C–O bond. The corresponding VB term has a weight of 30%, as seen in Chart III. We see in Figure 5 that spin polarization yields two opposite spins on the terminal carbon atom and on Fe, thus allowing for the direct formation of a second C–Fe bond. This way, a single adiabatic surface drives the system from the reactants to the metallacycle without necessarily passing through the formation of a stable intermediate. This finding contrasts with the case of Fe^{IV}–O and suggests that in the latter case, paths c and d are linked and that the formation of a metallacycle would occur with retention of the alkene stereochemistry. A remark must be made: the analysis of the same series of events in MO and state terms is tedious, since we would have to take into account the fact that the GS of the starting system is degenerate. The degeneracy is split upon interaction with C_2H_4, and we are left with two surfaces in spite of one in the case of Fe^{IV}–O. The VB approach reaches the essential features in a much more simple way.

Conclusion: Comparison with Experiment

Character of the Oxygen Atom in Fe^{IV}–O. The VB description of ferryl complexes reveals an important radical character for the oxygen atom and accounts for the observed "electrophilic" reactivity of these species,[5] at least to a large extent. The analogy with reactions of RO^0, rather than those with ionic species, must be outlined. The theoretical study shows that along the various reaction paths, *one-electron-transfer mechanisms are likely to occur.*

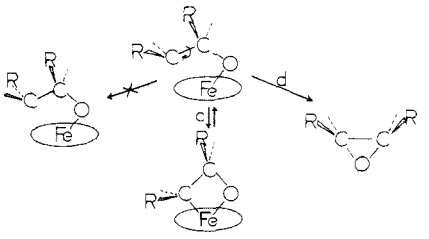

Figure 6. Proposed reaction scheme.

Nature of the Intermediate. In the case of Fe^{IV}–O, the covalent radical intermediate Fe–O–C–C^0 is prevented from spontaneous evolution by the existence of small potential energy barriers along all its potentially reactive channels. It might therefore exist as a transient species whose lifetime and competitive evolution will be ruled by the relative facilities of overcoming these barriers. At our level of investigation, it is not possible to quantify these possibilities. We have seen in the discussion that the presence of a porphyrin ring might bring about steric constraints, preventing the metallacycle formation from occurring. The octahedral geometry around Fe constitutes a major stabilization factor for the cycle. In systems possessing more degrees of freedom, the metallacycle formation according to path c is more likely to take place. Our results also suggest that ethylene oxide formation is obtained from the open intermediate, rather than from reductive elimination of the metallacycle. The obtention of the latter species remains to be experimentally investigated.

Possible Side Reactions of the Open Intermediate. If this species has a sufficient lifetime, it might be able to find out other ways of reacting. Specially, the radical carbon extremity might attack the porphyrin ring, forming new classes of complexes, as observed in some cases.[37] This kind of possibility is also at the origin of another pathway leading to *N*-alkylporphyrins (green pigment), reported by O. de Montellano[38] as a toxic event in the metabolism of terminal olefins by cytochrome P-450. Moreover, the intermediate might also yield aldehydes or ketones, as recently shown with psudomonas oleovarans,[39] cytochrome P-450,[40,15a] and heme models.[15]

Stereochemical Considerations. The stereochemical implications of the overall reactivity scheme are not easily stated, for we have seen that they result from the competition between various energy barriers found along the RCs and also from the relative facility of rotation around the central C–C bond. The observed stereospecificity of oxidations performed by the C_6H_5IO/Fe porphyrin system suggests that the latter type of barrier is the most important. This could be due to the steric hindrance of the porphyrin substituents which prevent the rotation around the central C–C bond. Accordingly, the epoxidation of stilbene by C_6H_5IO plus a nonrigid Fe catalyst is not stereospecific.[27] Moreover, it has been recently observed that the epoxidation stereoselectivity by oxomanganese porphyrins is enhanced by using bulky substituted porphyrins.[41,42] The ring substituents also modulate the relative

(37) Mansuy, D.; Battioni, J. P.; Akhrem, I.; Dupré, D.; Fisher, J.; Weiss, R.; Morgenstern-Badareau, I. *J. Am. Chem. Soc.* **1984**, *105*, 6112.
(38) (a) Ortiz de Montellano, P. R.; Mangold, B. L. K.; Wheeler, C.; Kunze, K. L.; Reich, N. O. *J. Biol. Chem.* **1983**, *258*, 4208. (b) Ortiz de Montellano, P. R.; Kunze, K. L.; Mico, B. A. *Molec. Pharmacol.* **1980**, *18*, 602.
(39) Katapodis, A. G.; Wimasalena, K.; Lee, J.; May, S. W. *J. Am. Chem. Soc.* **1984**, *106*, 7928.
(40) Liebler, D. C.; Guegenrich, F. P. *Biochemistry* **1983**, *22*, 5482.
(41) Bortoloni, O.; Meunier, B. *J. Chem. Soc., Perkin Trans. 2* **1984**, 1967.
(42) (a) Groves, J. T.; Kruper, W. J.; Haushalter, R. C. *J. Am. Chem. Soc.* **1980**, *102*, 6375. (b) Fontecave, M.; Mansuy, B. *Tetrahedron* **1984**, *40*, 4297. (c) Meunier, B.; Guilmet, E.; de Carvalho, M. E.; Poilblanc, R. *J. Am. Chem. Soc.* **1984**, *106*, 6668 and references cited therein.
(43) Hiberty, P. C. *Int. J. Quantum Chem.* **1981**, *19*, 259.

Table I. Calculated EHT Coefficients for π and π^*. Two Values of the ∠O–Fe–H Angles Are Given[a]

atomic AOs	∠O–Fe–H = 90°		∠O–Fe–H = 107.5°	
	π_x	π_x^*	π_x	π_x^*
O				
$2p_x$	0.8210	−0.5261	8.8170	−0.4818
Fe				
$3d_{xz}$	0.3450	0.9114	0.4347	0.8716
$4p_x$	0.0882	0.0001	0.0170	0.1856
H_1	0.1713	−0.1056	0.1248	−0.2576
H_2	−0.1713	0.1056	−0.1248	0.2576

[a] Only one component, relative to the xz (x) plane is given.

reactivity of cis and trans alkenes. Molecular models show that the previously described approach of the reactants exhibits nonbonded interactions between the olefin substituents and those of the ring, the constraint being greater in the case of trans compounds, thus explaining the better yields obtained for cis derivatives.[5g] The cis/trans selectivity is no longer observed for the nonrigid $FeCl_3/C_6H_5IO$ system.[27] The general scheme of Figure 6 summarizes all these possibilities in very good agreement with a study by Collman et al.[45] which appeared during the preparation of this paper.

Role of the Metal. A general comparison of various isoelectronic metals is not realistic at our level of modelization. Moreover, in this study we have only examined the oxygen-transfer reaction. It is clear that in real systems, however, this path only constitutes an event in a complex chain, whose rate-determining step is not well-known. Further, more quantitative studies are necessary in this field, and our goal was to promote the interest of both experimental and theoretical chemists for these series of reactions.

Appendix

EHT MOs can be used for building Slater determinants: $\Phi = NA|\Psi_1\bar{\Psi}_1\Psi_2\bar{\Psi}_2.....|$ where N is a normalization factor and A the antisymmetrization operator. It has been shown that a determinantal wave function describing any number of weakly interacting groups of electrons, for examples, depending on two fragments A and B, can be written, in the limit of zero interaction between A and B: $\Phi = NA|\Psi_A(\chi_{a1}.....\chi_{an})||\Psi_B(\chi_{b1}.....\chi_{bm})|$ where χ_{ai} and χ_{bj} belong to A and B, respectively. We thus obtain a generalized product of functions, and each determinant of the product describes, to a very good approximation, the behavior of the group of electrons to which it refers. A typical use of this method consists of treating separately the π system of a polyene whose relevant electrons are regarded as moving in the effective field of the rest of the molecule. This type of partition can be used for our model structures. Let us consider the MOs of L_4FeO. By order of increasing energy, we have, within the C_{4v} notation, $\Phi = NA|(1a_1)^2(2a_1)^2(1b_1)^2(1e)^4(3a_1)^2(2e)^4(1b_2)^2(3e)^2|$. The MOs of 1e and 3e are mainly located on O and Fe as shown in Table I, while those of 2e contain major contributions of the ligands with small O and Fe terms. The approximation lies in the consideration that the coupling between the elements of 2e and 1e + 3e is weak. Collecting the MOs, we get the new product $\Phi = NA'|(1a_1)^2(2a_1)^2(1b_1)^2(3a_1)^2(2e)^4(1b_2)^2|A''|(1e)^4(3e)^2|$. The smallest determinant describes the behavior of six electrons shared by Fe and O in the field of the rest of the porphyrin.

Table II. Wave Functions and Symmetries for the Case of Six and Five Electrons in Two Planes. These Functions Have Been Used for Calculating the VB Structures of Figure 3[a]

state	wave function in terms of π_+/π_-	real wave function
$^3A_2$	$\lvert\pi_+\bar{\pi}_+\pi_-(\pi_+^*\bar{\pi}_-^* - \pi_-^*\bar{\pi}_+^*)\rvert$	$\lvert\pi_x\bar{\pi}_x\pi_y(\pi_y^*\bar{\pi}_x^* - \pi_x^*\bar{\pi}_y^*)\rvert$
$^1B_2$	$\lvert\pi_+\bar{\pi}_+\pi_-\bar{\pi}_-(\pi_+^*\bar{\pi}_+ - \pi_-^*\bar{\pi}_-^*)\rvert$	$\lvert\pi_x\bar{\pi}_x\pi_y\bar{\pi}_y(\pi_x^*\bar{\pi}_y^* + \pi_x^*\bar{\pi}_y^*)\rvert$
$^1A_1$	$\lvert\pi_+\bar{\pi}_+\pi_-\bar{\pi}_-(\pi_+^*\bar{\pi}_- + \pi_-^*\bar{\pi}_+^*)\rvert$	$\lvert\pi_x\bar{\pi}_x\pi_y\bar{\pi}_y(\pi_x^*\bar{\pi}_x^* + \pi_y^*\bar{\pi}_y^*)\rvert$
$^1B_1$	$\lvert\pi_+\bar{\pi}_+\pi_-\bar{\pi}_-(\pi_+^*\bar{\pi}_+^* - \pi_-^*\bar{\pi}_-^*)\rvert$	$\lvert\pi_x\bar{\pi}_x\pi_y\bar{\pi}_y(\pi_x^*\bar{\pi}_x^* - \pi_y^*\bar{\pi}_y^*)\rvert$
$^3A_2^*$	$\lvert\pi_+\bar{\pi}_+\pi_-^*\bar{\pi}_-^*(\pi_-\bar{\pi}_+^* - \pi_+^*\bar{\pi})\rvert -$ $\lvert\pi_-\bar{\pi}_-\pi_+^*\bar{\pi}_+^*(\pi_+\bar{\pi}_-^* - \pi_-^*\bar{\pi}_+)\rvert$	$\lvert\pi_x\bar{\pi}_x\pi_y^*\bar{\pi}_y^*(\pi_y\bar{\pi}_x^* - \pi_x^*\bar{\pi}_y)\rvert -$ $\lvert\pi_y\pi_y\pi_x^*\bar{\pi}_x^*(\pi_x\bar{\pi}_y^* - \pi_y^*\bar{\pi}_x)\rvert$
^2E	$\lvert\pi_+\bar{\pi}_+\pi_-\bar{\pi}_-\pi_+^*\rvert$	$\lvert\pi_x\bar{\pi}_x\pi_y\bar{\pi}_y\pi_x^*\rvert + i\lvert\pi_x\bar{\pi}_x\pi_y\bar{\pi}_y\pi_y^*\rvert$

[a] The doublet state ^2E contains real and imaginary parts which have to be treated separately. In fact only one component is necessary, since the other can be deduced by evident symmetry. The normalization coefficients are omitted.

Let us focus our attention on the 6 × 6 determinant, $\Delta(6)$. Upon convenient rotation of the calculated MOs, one gets the equivalent set of degenerate MOs composed of $\pm 2p_x(O) + 3d_{xz}(Fe) + 4p_x(Fe)$ and $\pm 2p_y(O) + 3d_{yz}(Fe) + 4p_y(Fe)$ contributions labeled

$$\pi_+ = \pi_x + i\pi_y \qquad \pi_+^* = \pi_x^* + i\pi_y^*$$

$$\pi_- = \pi_x - i\pi_y \qquad \pi_-^* = \pi_x^* - i\pi_y^*$$

Using this notation, we have the determinantal wave functions of Table II where the correspondance between real and imaginary parts is given. Any of these functions can be written as $\pi = C_O[2p(O)] + C_{Fe}[d'(Fe)]$ where d′ is an appropriate 3d + 4p hybrid. Looking at the relative values of C_O and C_{Fe} in Table I, we finally can write, taking apart a multiplicative factor

$$\pi = 2p(O) + \alpha[d'(Fe)]$$

$$\pi^* = \alpha'[2p(O)] - d'(Fe)$$

where α and α' are very close to 0.5. A further simplification arises if we take $\alpha = \alpha'$, which is still in the order of approximation of the method. The resultant analytical forms are then injected in the wave functions of Table II, and the corresponding products are worked out. Upon examination of one component of $\Delta(6)$, say $\det|\pi_x(1)\bar{\pi}_x(2)\pi_y(3)\bar{\pi}_y(4)\pi_x^*(5)\bar{\pi}_y^*(6)|$, it is convenient to group the product according to spin separation as described by Hiberty and Leforestier,[43,44] yielding $\det|\pi_x(1)\pi_y(3)\pi_x^*(5)\bar{\pi}_x(2)\bar{\pi}_y(4)\bar{\pi}_y^*(6)|$. We just have to treat separately products of three terms. The size of the problem does not impose heavy calculations, and the determinants can be worked out readily. The results are given in Charts II and III as functions of α with indicative values of the coefficients normalized to unity, obtained for $\alpha = 0.5$.

Registry No. Ethylene, 74-85-1.

(44) Hiberty, P. C.; Leforestier, C. *J. Am. Chem. Soc.* **1978**, *100*, 2012.
(45) Collman, J. P.; Brauman, J. I.; Meunier, B.; Hayashi, T.; Kodadek, T.; Raybuck, S. A. *J. Am. Chem. Soc.* **1985**, *107*, 2000.